Model-Based Estimation of Ankle Joint Stiffness During Dynamic Tasks: a Validation-Based Approach

Christopher P. Cop[1], Guillaume Durandau[1], Alejandro Moya Esteban[1], Ronald C. van 't Veld[1], Alfred C. Schouten[1,2], and Massimo Sartori[1]

***Abstract*— Joint stiffness estimation under dynamic conditions still remains a challenge. Current stiffness estimation methods often rely on the external perturbation of the joint. In this study, a novel 'perturbation-free' stiffness estimation method via electromyography (EMG)-driven musculoskeletal modeling was validated for the first time against system identification techniques. EMG signals, motion capture, and dynamic data of the ankle joint were collected in an experimental setup to study the ankle joint stiffness in a controlled way, i.e. at a movement frequency of 0.6 Hz as well as in the presence and absence of external perturbations. The model-based joint stiffness estimates were comparable to system identification techniques. The ability to estimate joint stiffness at any instant of time, with no need to apply joint perturbations, might help to fill the gap of knowledge between the neural and the muscular systems and enable the subsequent development of tailored neurorehabilitation therapies and biomimetic prostheses and orthoses.**

I. INTRODUCTION

Joint stiffness is a mechanical property that is, in most of the cases, subconsciously modulated in humans across movements [1]. This modulation allows us to naturally adapt to different terrains and conditions [2]. Even though joint stiffness has been extensively investigated in the past decades [3], its regulation mechanisms are not completely understood yet. The dependency of this mechanical property on loading conditions, muscle contractile properties and neural control strategies represent a challenge for its estimation *in vivo*. Moreover, the availability of different definitions of joint stiffness make it difficult to develop a generic formulation for stiffness estimation [4]. Two examples of formulations of joint stiffness include short-range stiffness (SRS) and quasi-stiffness.

SRS is only valid during isometric muscle contractions. During dynamic conditions (i.e. dynamic stiffness) joint stiffness has been widely investigated using the notion of quasi-stiffness, which is easily calculated by computing the derivative of the joint torque-angle curve with respect to the angle. However, quasi-stiffness is only equivalent to joint stiffness in passive conditions, i.e. without muscle activation [5]. Therefore, methods that take into account the specific movement and muscle activation are necessary to derive dynamic, i.e. non-static, joint stiffness.

During the last decades, effort has been made to quantify joint stiffness, especially on the ankle joint because of its crucial role during locomotion. This effort is justified by the desire to gain a better understanding of human motor control both in healthy and diseased individuals, the need to devise personalized rehabilitation treatments or the ability to produce biomimetic actuated prostheses and orthoses [6].

Several techniques have been proposed to study dynamic joint stiffness: ultrasound elastography, system identification, and musculoskeletal modeling.

Ultrasound elastography can characterize tissue mechanical properties *in vivo* by measuring the deformation caused by an external stress or force [7]. This is enabling the study of muscle and tendon stiffness at the tissue level during isometric conditions, but stiffness measurements at the joint level still remain a challenge.

System identification has been employed extensively to estimate joint stiffness in isometric or postural conditions. Dynamic conditions, e.g. human gait, are the current focus of study [8]. Even though there exist many developed system identification algorithms, there is a common characteristic all methods share: the external perturbation of the joint [9]. The presence of a perturbation (produced by a robotic platform or a wearable robot) makes it difficult to perform physiological and natural movements, not to mention the complications associated to applying these perturbations on weaker individuals, e.g. patients suffering from stroke or spinal cord injury. Moreover, to integrate stiffness estimates in wearable robot controllers, the ability of decoding stiffness from bioelectrical signals would be desired.

Musculoskeletal modeling has been widely used to analyze the biomechanics of a variety of functional tasks *in silico*. Electromyography (EMG)-driven musculoskeletal modeling uses EMG recordings to *drive* musculoskeletal models [10], providing more realistic simulations from a physiological point of view. EMG-driven musculoskeletal modeling allows the estimation of joint stiffness during dynamic tasks without the need of perturbing the joint [3].

In this study, we present an EMG-driven ankle musculoskeletal model and validate it against system identification techniques in a controlled dynamic ankle stiffness estimation experiment. To the best of our knowledge, a comparison of system identification techniques and EMG-driven musculoskeletal modeling on the same dataset to estimate dynamic joint stiffness has never been done before. This provides an

*This work was partly funded by the ERC Starting Grant INTERACT (803035) and the Netherlands Organisation for Scientific Research (NWO), domain Applied and Engineering Sciences projects 14903 and 522234

[1]Department of Biomechanical Engineering, University of Twente, Enschede, The Netherlands c.p.cop@utwente.nl, m.sartori@utwente.nl

[2]Department of Biomechanical Engineering, Delft University of Technology, Delft, The Netherlands

978-1-5386-1311-5/19/$31.00 ©2019 IEEE

experimental, theoretical and computational framework for extending model-based methods for stiffness estimation.

II. METHODS

A. Data collection

Five healthy subjects (age: 24.2 $\pm$ 1.0 years; weight: 70.0 $\pm$ 5.4 kg; height: 1.78 $\pm$ 0.06 m) participated in this study. The Ethical Committee of the University of Twente approved all experimental procedures and all particpants gave written informed consent. The Achilles Rehabilitation Device (MOOG, Nieuw-Vennep, The Netherlands), an admittance controlled single axis manipulator, was used to measure the ankle joint's position and torque during dynamic trials. Motion capture data were acquired using a Visualeyez II tracker (PTI, Vancouver, Canada) at 100 Hz. EMG activity was recorded at 2048 Hz by the Porti system (TMSi, Oldenzaal, The Netherlands). The main elements of the experimental setup can be seen in Fig. 1.

Position tasks (i.e. dynamic) were performed using the Achilles Rehabilitation Device. In the rest of this manuscript, the term Achilles device will be used to refer to it. Subjects were asked to follow sinusoidal position targets with an amplitude of 0.15 rad at 0.6 Hz, both in unperturbed and perturbed conditions. The perturbations consisted of rotations of 0.03 rad with a switching time of 0.15 s that were pseudo-randomly applied to the ankle joint by the Achilles device.

The Achilles device was configured to reproduce a virtual inertia, damping, and stiffness of 1 kg·m^2, 2.5 N·m·s·rad^{-1}, and 60 N·m·rad^{-1}, respectively. These parameters rendered a viscoelastic virtual environment that made the Achilles device resist movement, contrary to what happens in minimal impedance mode, i.e. the controller follows the user and behaves as a "transparent" device.

Based on what was done in [3], the EMG data were acquired from five lower leg muscles: tibialis anterior, soleus, gastrocnemius medialis and lateralis, and peroneus longus. EMG linear envelopes were obtained after band-pass filtering (30-300 Hz), full-wave rectifying, and low-pass filtering (6 Hz) raw EMG signals using a zero-lag second-order Butterworth filter [3]. Three maximum voluntary contraction (MVC) trials were performed by each subject to normalize the EMG linear envelopes.

Motion capture data were recorded using 12 optical markers placed on the subjects' right leg. Several bony landmarks (i.e. greater trochanter, lateral epicondyle of the femur, head of the fibula, lateral malleolus, calcaneus, and the fifth metatarsal bone) were used for scaling a generic lower limb model [11]. In addition to the markers on the bony landmarks, three markers on the thigh and three markers on the shank were used to track the knee and ankle angles during the whole experiment.

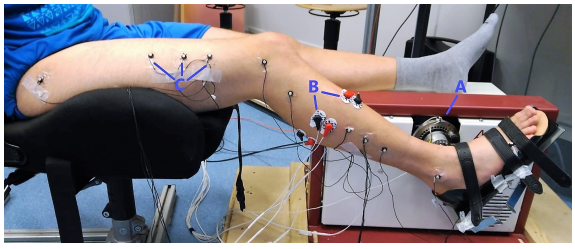

Fig. 1. Experimental setup. The Achilles Rehabilitation Device (A) was used to perturb and track the kinematics and dynamics of the ankle joint. Muscle activity (B) was recorded by the Porti system. Visualeyez optical LED markers (C) were used to capture the knee and ankle angles.

B. EMG-driven musculoskeletal modeling pipeline and dynamic stiffness computation

The open-source software OpenSim [12] was used to perform inverse kinematics on optical marker data to obtain joint angles, and to obtain the moment arms of the different musculotendon units (MTUs). The open-source toolbox Calibrated EMG-Informed Neuromusculoskeletal Modelling (CEINMS) [13] was used to estimate the ankle torque and the force of the MTUs as a function of recorded EMGs and joint angles and moment arms generated by OpenSim (Fig. 2). The model was firstly scaled using optical marker data and calibrated on the experimental torque recordings. The computed MTU variables were further used for dynamic stiffness computation. For a detailed description of the EMG-driven musculoskeletal modeling pipeline, the reader is referred to [10].

The stiffness model developed and described by Sartori et al. [3] was adapted and used to estimate the ankle joint stiffness (K^A). This model follows a bottom-up approach to obtain joint stiffness. This means that the stiffness estimations of muscle fibers and tendons are projected to the MTU

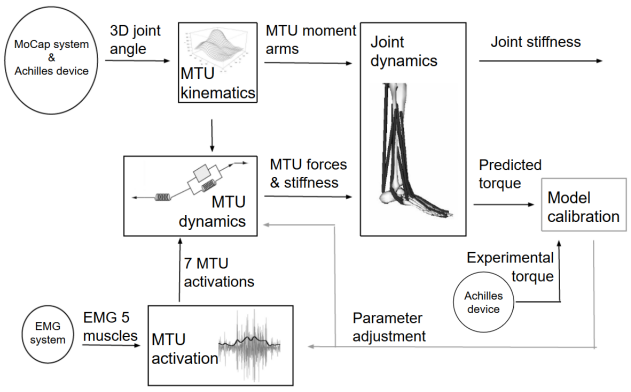

Fig. 2. Schematic diagram of the EMG-driven musculoskeletal modeling pipeline used in this study. It consists of five blocks: model calibration, MTU activation, MTU kinematics, MTU dynamics, and joint dynamics. Firstly, the model calibration block uses EMG-signals, three-dimensional (3D) joint angles and experimental ankle torques from several calibration trials to find the optimal set of model parameters that minimize the error between reference and computed torques. Once the model is calibrated, it is run in open-loop (i.e. the experimental ankle torque is no longer needed). The MTU activation block maps the EMG activity recorded from five muscles to non-linear activations of seven MTUs (peroneus brevis and peroneus tertius were also modeled). The MTU kinematics block derives MTU lengths and moment arms from experimental 3D ankle angles. MTU force and stiffness are computed as a function of MTU activation and MTU kinematics in the MTU dynamics block. Lastly, the joint torque and stiffness are obtained by projecting the resulting MTU forces and stiffness on the ankle plantar-dorsi flexion degree of freedom in the joint dynamics block. Figure adapted from [3].

level. Then, the stiffness of each MTU is projected to the joint level. A complete description of this stiffness model can be found in [3].

C. Data analysis

The EMG-driven model was validated at both the torque and the stiffness levels for the first time. At the torque level, ankle torques estimated by the model were compared to the experimental torques measured by the Achilles device. Results were compared both in shape and magnitude by the coefficient of determination (R^2) and the root mean squared error (RMSE), respectively.

At the stiffness level, stiffness estimations from the EMG-driven model were compared to the stiffness obtained by system identification techniques. The stiffness estimation via system identification on the same dataset was computed using a closed-loop ensemble-based system identification algorithm [9]. Results were compared both in shape and magnitude by the R^2 and the RMSE normalized with respect to the maximum stiffness (nRMSE), respectively. Additionally, to include a more global feature to compare results, an estimate of the total amount of ankle stiffness in each condition was defined as the area under the curve (AUC) of the stiffness profile.

III. RESULTS

Across all cycles (2060 in total), estimated torques were compared to the experimental torques to check the dynamical consistency of the EMG-driven musculoskeletal model (Fig. 3). R^2 values ranged from 0.60 to 0.98 (mean value = 0.93; standard deviation = 0.03). RMSE values ranged from 0.8 N·m to 5.1 N·m (mean value = 2.1 N·m; standard deviation = 0.6 N·m).

Our stiffness estimations were compared to the ones obtained via system identification. The results of all subjects were averaged (Fig. 4). Numerical values of this comparison are presented in Table I. In this experiment, R^2 and nRMSE values were 0.47 and 0.18, respectively. AUC values were also in agreement: 1251 N·m·rad^{-1} and 1240 N·m·rad^{-1} for EMG-driven modeling and system identification, respectively. Additionally, 76% of the average stiffness values obtained by the EMG-driven model were within a standard deviation interval of the mean stiffness value obtained via system identification.

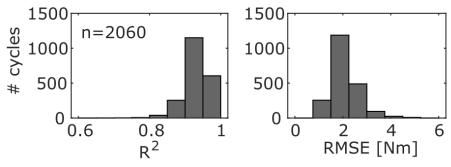

Fig. 3. Distribution of goodness-of-fit indices computed from experimental and modeled ankle torques across all cycles (n = 2060). Goodness-of-fit indices include the coefficient of determination (R^2) and the root mean squared error (RMSE). Histograms gather the R^2 and RMSE values in eight intervals with a fixed width in the (0.6, 1) and (0, 6) ranges, respectively.

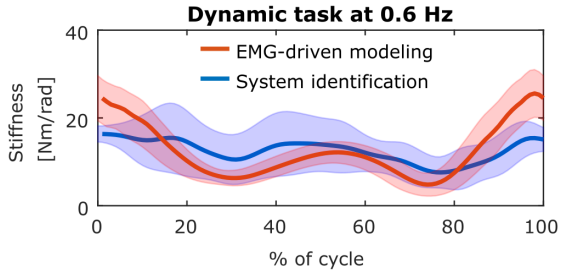

Fig. 4. Comparison of the stiffness estimations of the proposed model against system identification techniques for the dynamic task at 0.6 Hz. The thick red line represents the average stiffness across cycles and subjects obtained by the EMG-driven model, and the red shaded area corresponds to its standard deviation. The thick blue line represents the average stiffness estimation via system identification, and the blue shaded area depicts its standard deviation.

TABLE I
COMPARISON OF STIFFNESS ESTIMATIONS VIA EMG-DRIVEN MODELING AND SYSTEM IDENTIFICATION

	Modeling	System ID
AUC [Nm/rad]	1251	1240
Max. Stiff. [Nm/rad]	26	16
Min. Stiff. [Nm/rad]	5	8
R^2	0.47	
nRMSE	0.18	

We could not observe clear differences between the perturbed and unperturbed trials among our model-based estimations.

IV. DISCUSSION

In this study we aimed to validate the dynamic stiffness model proposed in [3] against system identification techniques in a controlled experiment. Additionally, the effects of external perturbations were investigated.

The validation of the EMG-driven musculoskeletal model at the torque level (Fig. 3) showed that the model was dynamically consistent and able to predict the joint torque satisfactorily.

At the stiffness level, however, differences between our proposed methodology and a system identification algorithm adapted for this specific experiment were greater. Since there is no golden standard in stiffness estimation, it is difficult to assess which results are closer to the real joint stiffness. It is important to mention that, whereas our model is able to predict instantaneous stiffness, the system identification algorithm needs many cycles to compute the stiffness estimation of a single period. Doing this, it assumes that the position, torque, and stiffness of the ankle joint are perfectly periodic, while our model is able to access instantaneous stiffness, taking unexpected changes in position and torque into account.

Results showed rather low stiffness peaks in dorsi-flexion (DF) (Fig. 4), likely due to fact that the model only included a sub-set of the ankle dorsi-flexor muscles, i.e. tibialis anterior and peroneus tertius. Future work will include all

DF muscles and evaluate the effect on stiffness estimation. Another reason for this low stiffness in DF may be wrongly calibrated MTUs with parameters that hit the pre-defined boundaries. Optimization algorithms such as the one presented by Modenese el al. [14] might improve the calibration of highly sensitive parameters such as the tendon slack lengths and the optimal muscle fiber lengths, which would most likely improve the overall performance of our model-based approach.

We did not observe significant differences between the perturbed and the unperturbed trials. Our model does not include history-dependent force generating mechanisms, such as SRS. SRS has an effect in the initial instants of time after the muscle fibers are being stretched or shortened, e.g. during an external perturbation. Future studies should implement a modification of the Hill-type muscle model to include SRS, as proposed by De Groote et al. in [15]. Additionally, the unperturbed trials were always performed before the perturbed ones. Therefore, it could be that the subjects were still adapting to the new condition in the unperturbed trial, which might have led to a stiffer response than expected.

Joint stiffness is a property that depends on the task that is being performed. Hence, comparison with international literature is complex since the experimental conditions were probably different. Nevertheless, our stiffness estimations are in line with other studies. Lee et al. [16] reported ankle stiffness values between 30 $\mathrm{N{\cdot}m{\cdot}rad^{-1}}$ and 60 $\mathrm{N{\cdot}m{\cdot}rad^{-1}}$ for different stages of the human gait cycle. Our estimations were roughly between 5 $\mathrm{N{\cdot}m{\cdot}rad^{-1}}$ and 30 $\mathrm{N{\cdot}m{\cdot}rad^{-1}}$.

Future systematic analyses must be conducted to investigate joint stiffness estimation across larger condition repertoires including different task velocities and loads. Additionally, the stiffness estimations for the different subjects were averaged in this study. Extensions of this work will investigate inter-subject variability.

Our proposed methodology possesses some limitations. We have seen that the calibration of model parameters is a sensitive step during the stiffness estimation process that still needs improvement. Additionally, not all the muscles spanning the ankle joint were included. Another limitation is that structures such as the skin and ligaments, which somehow contribute to the global joint stiffness, are not modeled. Moreover, certain stages of the experiment, such as sensor placement, MVC trials or model scaling, are dependent on the subject or the investigator and are therefore an important source of uncertainties. Lastly, problems associated to the utilization of single-channel surface EMG electrodes, such as cross-talk, may be solved by using high density EMG electrodes in conjunction with decomposition techniques [17]. This would allow to drive individual motor units with a high spatial resolution.

Being able to access instantaneous dynamic joint stiffness will have tremendous implications in understanding human movement, as well as the development of tailored neurorehabilitation therapies and biomimetic control of prostheses [18] and orthoses [19].

REFERENCES

[1] B. J. Misgeld, T. Zhang, M. J. Lüken, and S. Leonhardt, "Model-based estimation of ankle joint stiffness," *Sensors*, vol. 17, no. 4, p. 713, 2017.

[2] T. Ogawa, N. Kawashima, T. Ogata, and K. Nakazawa, "Predictive control of ankle stiffness at heel contact is a key element of locomotor adaptation during split-belt treadmill walking in humans," *Journal of neurophysiology*, vol. 111, no. 4, pp. 722–732, 2013.

[3] M. Sartori, M. Maculan, C. Pizzolato, M. Reggiani, and D. Farina, "Modeling and simulating the neuromuscular mechanisms regulating ankle and knee joint stiffness during human locomotion," *Journal of neurophysiology*, vol. 114, no. 4, pp. 2509–2527, 2015.

[4] M. L. Latash and V. M. Zatsiorsky, "Joint stiffness: Myth or reality?" *Human movement science*, vol. 12, no. 6, pp. 653–692, 1993.

[5] E. J. Rouse, R. D. Gregg, L. J. Hargrove, and J. W. Sensinger, "The difference between stiffness and quasi-stiffness in the context of biomechanical modeling," *IEEE Transactions on Biomedical Engineering*, vol. 60, no. 2, pp. 562–568, 2013.

[6] M. Sartori, D. G. Llyod, and D. Farina, "Neural data-driven musculoskeletal modeling for personalized neurorehabilitation technologies," *IEEE Transactions on Biomedical Engineering*, vol. 63, no. 5, pp. 879–893, 2016.

[7] S. F. Eby, P. Song, S. Chen, Q. Chen, J. F. Greenleaf, and K.-N. An, "Validation of shear wave elastography in skeletal muscle," *Journal of biomechanics*, vol. 46, no. 14, pp. 2381–2387, 2013.

[8] H. Lee, E. J. Rouse, and H. I. Krebs, "Summary of human ankle mechanical impedance during walking," *IEEE journal of translational engineering in health and medicine*, vol. 4, pp. 1–7, 2016.

[9] D. Ludvig, M. Plocharski, P. Plocharski, and E. J. Perreault, "Mechanisms contributing to reduced knee stiffness during movement," *Experimental brain research*, vol. 235, no. 10, pp. 2959–2970, 2017.

[10] M. Sartori, M. Reggiani, D. Farina, and D. G. Lloyd, "Emg-driven forward-dynamic estimation of muscle force and joint moment about multiple degrees of freedom in the human lower extremity," *PloS one*, vol. 7, no. 12, p. e52618, 2012.

[11] S. L. Delp, J. P. Loan, M. G. Hoy, F. E. Zajac, E. L. Topp, and J. M. Rosen, "An interactive graphics-based model of the lower extremity to study orthopaedic surgical procedures," *IEEE Transactions on Biomedical engineering*, vol. 37, no. 8, pp. 757–767, 1990.

[12] S. L. Delp, F. C. Anderson, A. S. Arnold, P. Loan, A. Habib, C. T. John, E. Guendelman, and D. G. Thelen, "Opensim: open-source software to create and analyze dynamic simulations of movement," *IEEE transactions on biomedical engineering*, vol. 54, no. 11, pp. 1940–1950, 2007.

[13] C. Pizzolato, D. G. Lloyd, M. Sartori, E. Ceseracciu, T. F. Besier, B. J. Fregly, and M. Reggiani, "Ceinms: A toolbox to investigate the influence of different neural control solutions on the prediction of muscle excitation and joint moments during dynamic motor tasks," *Journal of biomechanics*, vol. 48, no. 14, pp. 3929–3936, 2015.

[14] L. Modenese, E. Ceseracciu, M. Reggiani, and D. G. Lloyd, "Estimation of musculotendon parameters for scaled and subject specific musculoskeletal models using an optimization technique," *Journal of biomechanics*, vol. 49, no. 2, pp. 141–148, 2016.

[15] F. De Groote, J. L. Allen, and L. H. Ting, "Contribution of muscle short-range stiffness to initial changes in joint kinetics and kinematics during perturbations to standing balance: A simulation study," *Journal of Biomechanics*, vol. 55, pp. 71–77, 2017.

[16] H. Lee and N. Hogan, "Time-varying ankle mechanical impedance during human locomotion," *IEEE Transactions on Neural Systems and Rehabilitation Engineering*, vol. 23, no. 5, pp. 755–764, 2015.

[17] M. Sartori, U. Ş. Yavuz, and D. Farina, "In vivo neuromechanics: Decoding causal motor neuron behavior with resulting musculoskeletal function," *Scientific reports*, vol. 7, no. 1, p. 13465, 2017.

[18] M. Sartori, G. Durandau, S. Došen, and D. Farina, "Robust simultaneous myoelectric control of multiple degrees of freedom in wrist-hand prostheses by real-time neuromusculoskeletal modeling," *Journal of neural engineering*, vol. 15, no. 6, p. 066026, 2018.

[19] G. Durandau, W. Rampeltshammer, H. Van Der Kooij, and M. Sartori, "Toward muscle-driven control of wearable robots: A real-time framework for the estimation of neuromuscular states during human-exoskeleton locomotion tasks," in *2018 7th IEEE International Conference on Biomedical Robotics and Biomechatronics (Biorob)*. IEEE, 2018, pp. 683–688.